

Distinct roles of GCN5/PCAF-mediated H3K9ac and CBP/p300-mediated H3K18/27ac in nuclear receptor transactivation

Qihuang Jin¹, Li-Rong Yu^{2,5},
Lifeng Wang^{1,5}, Zhijing Zhang³,
Lawryn H Kasper⁴, Ji-Eun Lee¹,
Chaochen Wang¹, Paul K Brindle⁴,
Sharon YR Dent³ and Kai Ge^{1,*}

¹Nuclear Receptor Biology Section, CEB, National Institute of Diabetes and Digestive and Kidney Diseases, National Institutes of Health, Bethesda, MD, USA, ²Center of Excellence for Proteomics, Division of Systems Biology, National Center for Toxicological Research, FDA, Jefferson, AR, USA, ³Department of Biochemistry and Molecular Biology, University of Texas MD Anderson Cancer Center, Houston, TX, USA and ⁴Department of Biochemistry, St Jude Children's Research Hospital, Memphis, TN, USA

Histone acetyltransferases (HATs) GCN5 and PCAF (GCN5/PCAF) and CBP and p300 (CBP/p300) are transcription co-activators. However, how these two distinct families of HATs regulate gene activation remains unclear. Here, we show deletion of GCN5/PCAF in cells specifically and dramatically reduces acetylation on histone H3K9 (H3K9ac) while deletion of CBP/p300 specifically and dramatically reduces acetylations on H3K18 and H3K27 (H3K18/27ac). A ligand for nuclear receptor (NR) PPAR δ induces sequential enrichment of H3K18/27ac, RNA polymerase II (Pol II) and H3K9ac on PPAR δ target gene *Angptl4* promoter, which correlates with a robust *Angptl4* expression. Inhibiting transcription elongation blocks ligand-induced H3K9ac, but not H3K18/27ac, on the *Angptl4* promoter. Finally, we show GCN5/PCAF and GCN5/PCAF-mediated H3K9ac correlate with, but are surprisingly dispensable for, NR target gene activation. In contrast, CBP/p300 and their HAT activities are essential for ligand-induced Pol II recruitment on, and activation of, NR target genes. These results highlight the substrate and site specificities of HATs in cells, demonstrate the distinct roles of GCN5/PCAF- and CBP/p300-mediated histone acetylations in gene activation, and suggest an important role of CBP/p300-mediated H3K18/27ac in NR-dependent transcription.

The EMBO Journal (2011) 30, 249–262. doi:10.1038/emboj.2010.318; Published online 3 December 2010

Subject Categories: chromatin & transcription

Keywords: CBP and p300; GCN5 and PCAF; histone acetylation; nuclear receptor

*Corresponding author. Nuclear Receptor Biology Section, CEB, National Institute of Diabetes and Digestive and Kidney Diseases, National Institutes of Health, Building 10, Room 8N307C, 9000 Rockville Pike, Bethesda, MD 20892, USA. Tel.: +1 301 451 1998;

Fax: +1 301 480 1021; E-mail: kaig@nidk.nih.gov

⁵These authors contributed equally to this work

Received: 23 June 2010; accepted: 5 November 2010; published online: 3 December 2010

Introduction

Histone modifications, in particular methylation (me) and acetylation (ac) on the lysine residues of core histones, have been implicated in regulating both global and inducible gene expression (Kouzarides, 2007; Li *et al.*, 2007). Histone methylation associates with both gene activation and repression, depending on the specific lysine (K) residue that gets methylated and the state of methylation (me1, me2 or me3) (Barski *et al.*, 2007; Kouzarides, 2007). For example, tri-methylations on K4 and K36 of histone H3 (H3K4me3 and H3K36me3) associate with gene activation. H3K4me3 is enriched around the transcription start sites (TSSs) and associates with serine 5-phosphorylated initiating RNA polymerase II (S5P Pol II). H3K36me3 is enriched at the 3' end of transcribed regions and associates with serine 2-phosphorylated elongating RNA Pol II (S2P Pol II). In contrast, both di-methylation on K9 of histone H3 (H3K9me2) and tri-methylation on K27 of histone H3 (H3K27me3) are associated with gene silencing (Kouzarides, 2007).

Histone acetylation generally correlates with gene activation, although the molecular mechanisms by which histone acetylation regulates transcription remain largely undetermined. Histone acetyltransferases (HATs) often are capable of acetylating multiple lysine (K) residues *in vitro*. Thus, the biological functions of histone acetylation are believed to largely rely on the cumulative effects (Li *et al.*, 2007). Genome-wide analyses of histone acetylation patterns in mammalian cells have confirmed the correlation between histone acetylation and gene activation. For example, H3K9ac, H3K18ac and H3K27ac are enriched around the TSSs while acetylations on histone H4 are enriched in both the promoters and the transcribed regions of active genes (Wang *et al.*, 2008b). However, it remains to be established whether the increased histone acetylations are a cause or a consequence of the increased transcription in mammalian cells (Roth *et al.*, 2001).

The identification of yeast GCN5 protein as the first transcription-related HAT provides strong molecular evidence to directly link histone acetylation and gene activation (Brownell *et al.*, 1996). Yeast GCN5 is the enzymatic subunit of the SAGA complex that is capable of acetylating multiple K residues on histone H3 *in vitro*, including H3K9, H3K14, H3K18 and H3K23 (Grant *et al.*, 1999). In contrast, the yeast NuA3 complex preferentially acetylates H3K14 (Lee and Workman, 2007). Mammals express two highly homologous GCN5-like paralogues: GCN5 and PCAF. Deletion of mouse GCN5 leads to early embryonic lethality, while PCAF knockout mice show no obvious phenotype. Combined loss of GCN5 and PCAF in mice leads to more severe developmental defects, suggesting a partial functional redundancy between GCN5 and PCAF *in vivo* (Roth *et al.*, 2001). GCN5 and PCAF exist, in a mutually exclusive manner, in the multi-subunit mammalian SAGA (also known as STAGA and TFTC) and

ATAC complexes. These two HAT complexes use GCN5 or PCAF as the acetyltransferase to specifically acetylate nucleosomal histone H3 *in vitro* (Wang *et al.*, 2008a).

The mammalian CBP and p300 are another pair of ubiquitously expressed, paralogous proteins that belong to a distinct family of HATs (Bedford *et al.*, 2010). CBP and p300 are both essential for animal development as deletion of either one in mice leads to early embryonic lethality. These two HATs have been shown to function as transcription co-activators for hundreds of transcription factors including nuclear receptors (NRs) (Kraus and Wong, 2002; Bedford *et al.*, 2010). CBP and p300 are largely functionally interchangeable *in vitro* and in cultured cells, but they also display unique properties *in vivo* (Kasper *et al.*, 2006). *In vitro*, CBP/p300 are capable of acetylating multiple K residues on core histones (Kouzarides, 2007).

Genome-wide mapping of HATs in human cells shows that consistent with their roles as transcription co-activators, both the GCN5/PCAF and the CBP/p300 pairs of HATs correlate with gene activation and are recruited to regions surrounding the TSSs (Wang *et al.*, 2009). However, the substrate and site specificities of mammalian GCN5/PCAF and CBP/p300 *in vivo*, as well as the roles of GCN5/PCAF- and CBP/p300-mediated histone acetylations in gene activation, remain largely unclear.

Ligand-induced activation of NR target genes provides a robust model system to study the molecular mechanisms underlying transcription regulation (Rosenfeld and Glass, 2001; Kraus and Wong, 2002). GCN5 has been shown to function as a transcription co-activator for several NRs such as androgen receptor, estrogen receptor α (ER α) and PPAR γ (Yanagisawa *et al.*, 2002; Zhao *et al.*, 2008). Similarly, PCAF has been shown to function as a co-activator for ER α , retinoic acid receptor (RAR) and thyroid hormone receptor (TR) on reporter genes (Blanco *et al.*, 1998; Korzus *et al.*, 1998). GCN5 and PCAF are enriched on ER α target gene promoters upon ligand treatment (Metivier *et al.*, 2003). However, the data that implicate GCN5/PCAF as NR co-activators were mostly obtained from ectopic expression of GCN5/PCAF in reporter assays. It remains to be determined whether GCN5/PCAF are required for activation of endogenous NR target genes. More importantly, the role of GCN5/PCAF-mediated histone acetylation in NR-dependent transcription is largely unclear.

The roles of CBP/p300 as NR co-activators are better characterized. CBP/p300 were initially shown to function as transcription co-activators for glucocorticoid receptor, RAR and TR on reporter genes in cells (Chakravarti *et al.*, 1996; Kamei *et al.*, 1996). p300 acts synergistically with ligand-activated ER α and RAR to enhance transcription initiation on chromatin templates *in vitro* (Kraus and Kadonaga, 1998; Dilworth *et al.*, 2000). Further, p300 requires its HAT activity to function as a co-activator for ER α and TR (Kraus *et al.*, 1999; Li *et al.*, 2000). CBP/p300 are also enriched on ER α target gene promoters upon ligand treatment (Metivier *et al.*, 2003). In both primary CBP^{+/-} cells and primary p300^{-/-} cells, NRs show reduced transcriptional activities on reporter genes (Yao *et al.*, 1998; Yamauchi *et al.*, 2002). These results indicate that CBP/p300 are important for ligand-induced NR target gene activation. However, likely due to the early embryonic lethality of both CBP^{-/-} and p300^{-/-} mice as well as the potential functional redundancy between CBP and

p300 in cells, the roles of CBP/p300 in expression of endogenous NR target genes were incompletely understood. More importantly, because the substrate and site specificities of CBP/p300 *in vivo* were not determined, the molecular mechanisms by which CBP/p300-mediated histone acetylations regulate NR-dependent transcription have remained largely unclear.

PPAR δ is a ubiquitously expressed NR. Activation of PPAR δ promotes fat burning. Highly specific synthetic PPAR δ ligands (agonists) such as GW501516 (GW), are promising drug candidates for obesity and diabetes (Evans *et al.*, 2004). Endogenous PPAR δ is abundantly expressed in mouse embryonic fibroblasts (MEFs), but associates with histone deacetylases and behaves as a transcriptional repressor in the absence of ligand. Upon ligand treatment, endogenous PPAR δ switches from a repressor to an activator, which leads to a robust activation of target genes (Shi *et al.*, 2002). *Angiotensin-like 4* (*Angptl4*, also known as *PGAR* and *FIAP*) is a direct target gene of PPAR δ , with the PPAR response element (PPRE) being located at 2.3 kb downstream of the TSS in intron 3 (Mandard *et al.*, 2004). Treating MEFs with 100 nM GW selectively activates PPAR δ target genes in MEFs, with *Angptl4* being the most significantly induced one (Oliver *et al.*, 2001; Hummasti and Tontonoz, 2006).

In this paper, we use the GW-induced *Angptl4* expression in MEFs as a model system to initiate the investigation on the roles of GCN5/PCAF- and CBP/p300-mediated histone acetylations in NR target gene activation. We found that GW induces sequential enrichment of H3K18/27ac, Pol II, H3K9ac, and several histone methylations on the *Angptl4* promoter. Using GCN5/PCAF double knockout (DKO) cells and CBP/p300 DKO cells, we determined the substrate and site specificities of these two distinct families of HATs in cells and show that GCN5/PCAF and CBP/p300 are specifically required for H3K9ac and H3K18/27ac, respectively. Surprisingly, GCN5/PCAF-mediated H3K9ac correlates with, but is dispensable for, GW-induced *Angptl4* expression. In contrast, CBP/p300 and their HAT activities are essential for both GW-induced enrichment of histone modifications and Pol II on the *Angptl4* promoter and GW-induced *Angptl4* expression. Examination of several other endogenous NR target genes obtained similar results.

Results

PPAR δ ligand-induced histone modifications on *Angptl4* gene

By quantitative reverse transcriptase-PCR (qRT-PCR) analysis of gene expression, we confirmed the PPAR δ ligand GW-dependent activation of known direct PPAR δ target genes *Angptl4* and *PDK4* in MEFs, with *Angptl4* being more significantly induced (Figure 1A; Supplementary Figure S1A). Consistent with the previous report that PPAR δ functions as a transcriptional repressor in the absence of ligand (Shi *et al.*, 2002), deletion of PPAR δ by retroviral Cre expression in PPAR δ ^{flox/flox} MEFs led to a moderate increase of the basal level of *Angptl4*. However, deletion of PPAR δ in MEFs completely prevented the GW-induced *Angptl4* and *PDK4* expression, indicating that ligand-induced expression of endogenous *Angptl4* and *PDK4* is strictly dependent on PPAR δ (Supplementary Figure S1A). Consistent with *Angptl4* and *PDK4* being direct target genes of PPAR δ , protein

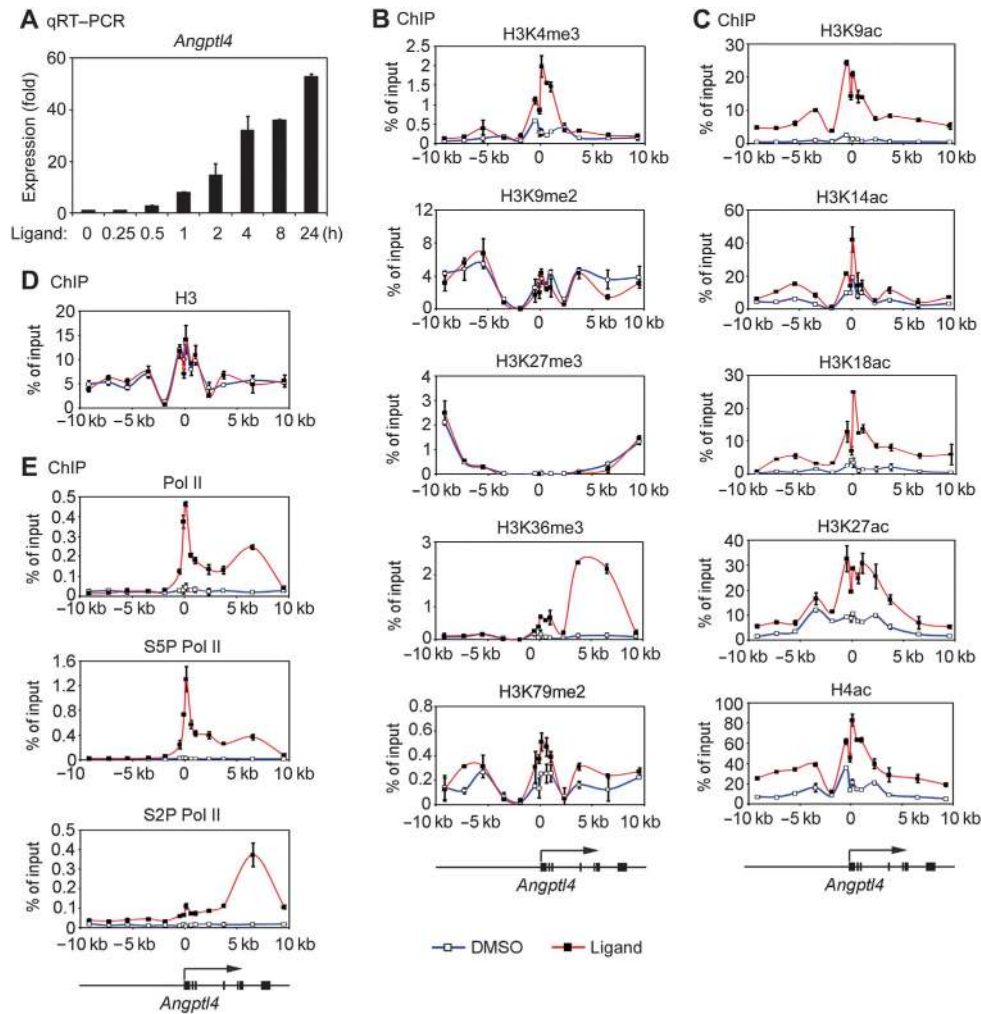


Figure 1 PPAR δ ligand-induced histone modifications on *Angptl4* gene. (A) Ligand-dependent activation of PPAR δ target gene *Angptl4* in MEFs. Wild-type MEFs were treated with 100 nM PPAR δ -specific ligand GW501516 (GW). Samples were collected at indicated time points for analysis of *Angptl4* expression by qRT-PCR. (B–E) MEFs were treated with GW or DMSO for 24 h, followed by chromatin immunoprecipitation (ChIP) analyses on *Angptl4* gene. The intron/exon organization of the 6.6-kb *Angptl4* gene is shown at the bottom with an arrow indicating the transcription start site. (B) ChIP of histone methylations using antibodies against H3K4me3, H3K9me2, H3K27me3, H3K36me3 and H3K79me2, respectively. (C) ChIP of histone acetylations using antibodies against H3K9ac, H3K14ac, H3K18ac, H3K27ac and H4ac, respectively. (D) ChIP of histone H3. (E) ChIP of total RNA polymerase II (Pol II), serine 5-phosphorylated initiating Pol II (S5P Pol II) and serine 2-phosphorylated elongating Pol II (S2P Pol II). All results are representative of two to four independent experiments. Quantitative PCR data in all figures are presented as mean values \pm s.d.

synthesis inhibitor cycloheximide failed to inhibit GW-induced *Angptl4* and *PDK4* expression in MEFs (Supplementary Figure S1B).

As the first step towards understanding the roles of histone modifications in regulating ligand-induced NR target gene expression, MEFs were treated with GW for 24 h, followed by chromatin immunoprecipitation (ChIP) analyses of histone modifications on the *Angptl4* gene. As shown in Figure 1B, GW treatment had little effect on the levels of H3K9me2 and H3K27me3 but increased H3K4me3, H3K36me3 and H3K79me2 signals on *Angptl4* gene, which correlated with the GW-induced *Angptl4* expression. GW-induced H3K4me3 and H3K79me2 were enriched around the TSS while GW-induced H3K36me3 was enriched at the 3' end of the transcribed region.

GW treatment increased the levels of all histone acetylations that we have examined on *Angptl4* gene, including

H3K9ac, H3K14ac, H3K18ac, H3K27ac and histone H4 acetylation (H4ac), with the signals peaked around the TSS (Figure 1C). The GW-induced histone methylations and acetylations were not due to change in nucleosome occupancy, as the histone H3 signal on *Angptl4* gene was not affected by GW treatment (Figure 1D).

We next examined the Pol II recruitment on *Angptl4* gene in GW-treated MEFs (Figure 1E). In the absence of GW, the signals of total Pol II, serine 5-phosphorylated initiating Pol II (S5P Pol II) and serine 2-phosphorylated elongating Pol II (S2P Pol II) were all very low on *Angptl4* gene. GW treatment led to markedly increased enrichment of all three types of Pol II on *Angptl4* gene. The signal of S5P Pol II peaked around the TSS while the signal of S2P Pol II peaked at the 3' end of the transcribed region. These results indicate that Pol II recruitment is a major regulatory step for PPAR δ ligand-induced *Angptl4* expression.

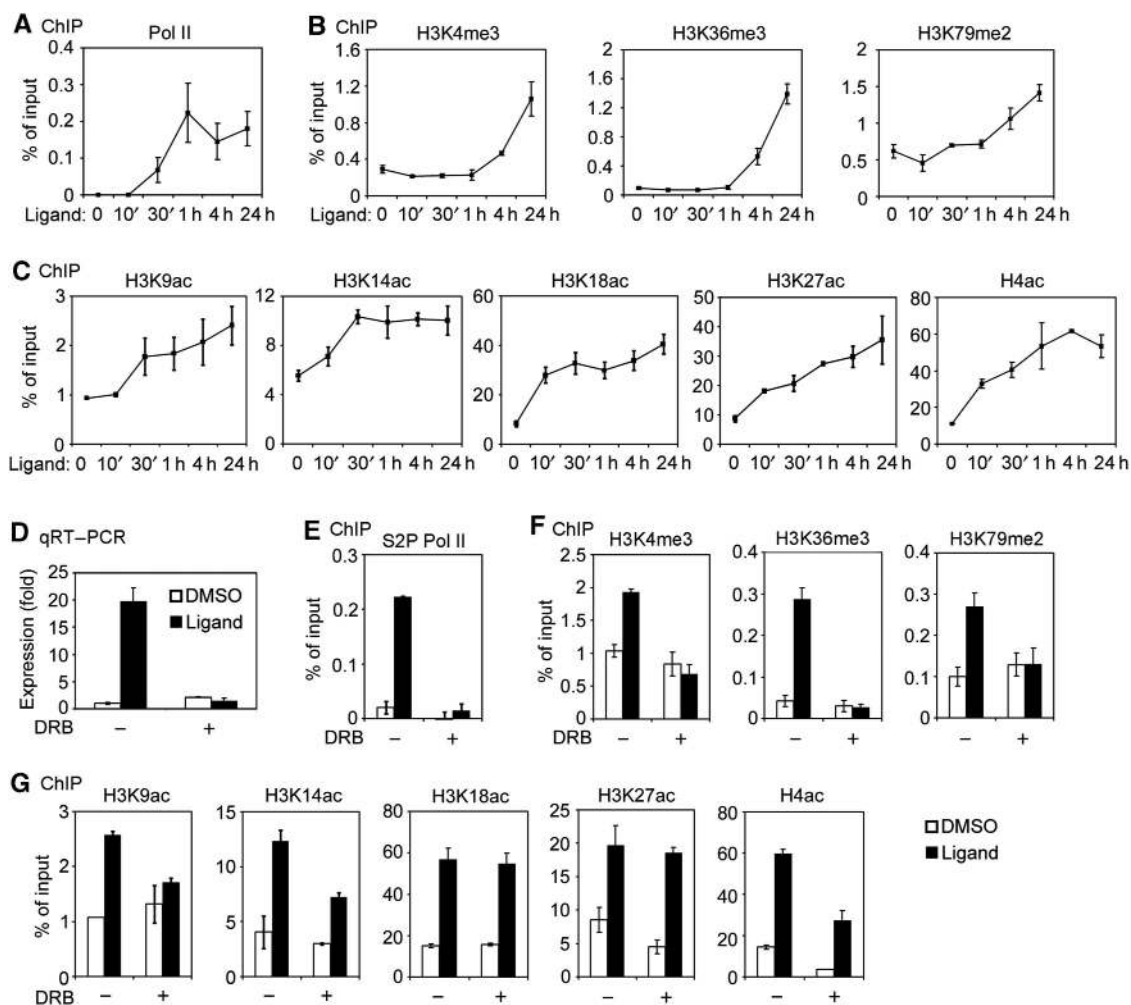


Figure 2 PPAR δ ligand induces sequential histone modifications on *Angptl4* gene. (A–C) The time courses of GW-induced Pol II recruitment and histone methylations and acetylations on *Angptl4* gene. Wild-type MEFs were treated with GW. Cells were collected at indicated time points for ChIP analyses of total Pol II (A), histone methylations (B) and acetylations (C) on *Angptl4* gene. (D–G) Wild-type MEFs were pre-treated with DRB for 30 min, followed by treatment with GW for 4 h in the presence of DRB. Cells were collected for analysis of *Angptl4* expression (D), as well as ChIP analyses of S2P Pol II (E), histone methylations (F) and acetylations (G) on *Angptl4* gene. Based on Figure 1, we chose the +3.7-kb and the +6.5-kb regions on *Angptl4* gene to examine GW-induced H3K36me3 and S2P Pol II, respectively. All other histone modifications and Pol II recruitment were examined at the +0.6-kb region on *Angptl4* gene. All results are representative of two to four independent experiments.

PPAR δ ligand induces sequential histone modifications on *Angptl4* gene

Next, we examined the time course of PPAR δ ligand-induced histone modifications and Pol II recruitment on *Angptl4* gene. MEFs were treated with GW for 0, 10, 30 min, 1, 4 and 24 h, followed by ChIP assays. Based on Figure 1 results, we chose the +3.7- and +6.5-kb regions on *Angptl4* gene to examine GW-induced H3K36me3 and S2P Pol II, respectively. Other histone modifications and Pol II recruitment were examined at the +0.6-kb region on *Angptl4* gene. As shown in Figure 2A–C, significantly increased H3K14ac, H3K18ac, H3K27ac and H4ac signals were observed on *Angptl4* gene 10 min after the start of GW treatment. The increased H3K9ac and Pol II signals were observed after 30 min while the increased H3K4me3, H3K36me3 and H3K79me2 signals observed after MEFs were treated with GW for 4 h.

To verify the sequential manner of GW-induced histone modifications on *Angptl4* gene, we used DRB, an inhibitor of transcription elongation (Edmunds *et al*, 2008). As prolonged

exposure to DRB is toxic to cells, we pre-treated MEFs with DRB for 30 min, followed by GW treatment in the presence of DRB for 4 h. DRB completely blocked GW-induced *Angptl4* expression (Figure 2D). Consistent with its role as an inhibitor of transcription elongation, DRB blocked enrichment of S2P Pol II to *Angptl4* gene (Figure 2E). DRB completely blocked GW-induced H3K9ac, H3K4me3, H3K36me3 and H3K79me2, and decreased GW-induced H3K14ac and H4ac, but had no effect on GW-induced H3K18ac and H3K27ac on *Angptl4* gene (Figure 2F and G). Thus, GW-induced H3K18ac and H3K27ac precede, while GW-induced H3K9ac, H3K4me3, H3K36me3 and H3K79me2 occur following the start of transcription elongation on *Angptl4* gene.

GCN5 and PCAF are specifically required for H3K9ac in cells

The dynamic histone H3 methylations and H4ac during gene induction have been investigated (Edmunds *et al*, 2008; Hargreaves *et al*, 2009). We decided to focus on the role of histone H3 acetylation in regulating ligand-induced NR target

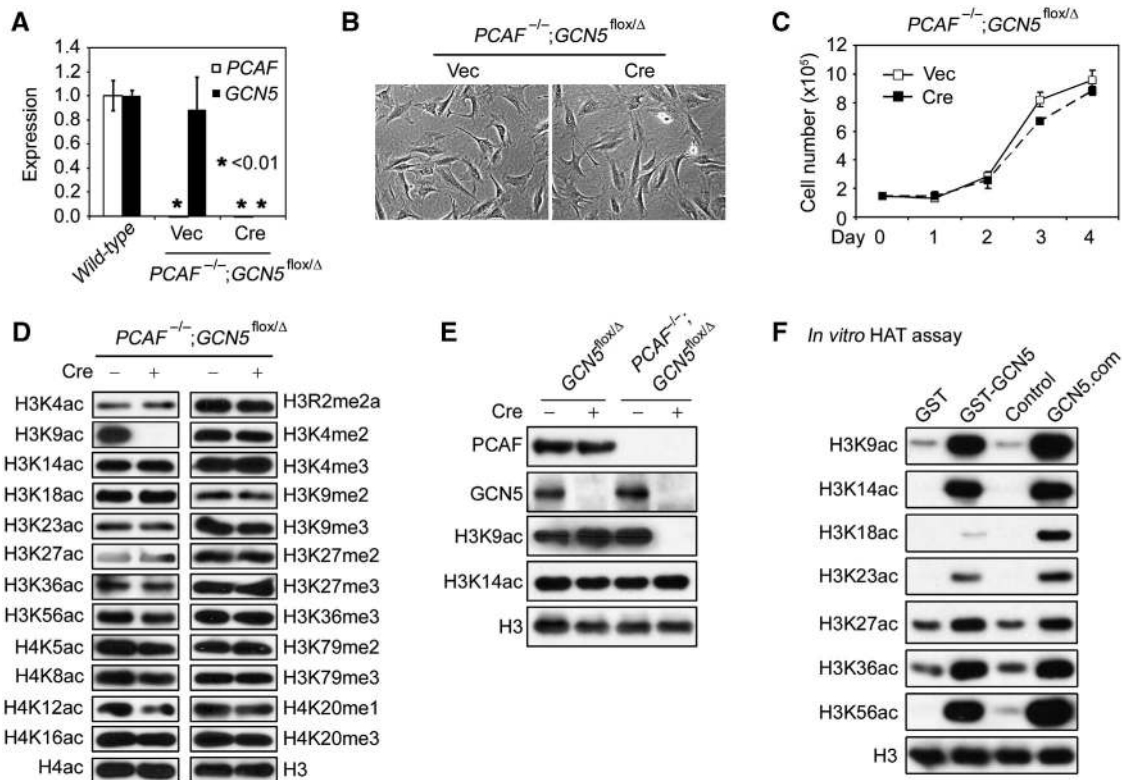


Figure 3 GCN5 and PCAF are redundant and are specifically required for H3K9ac in cells. Immortalized *PCAF*^{-/-}; *GCN5*^{fllox/Δ} MEFs were infected with retroviruses MSCVpuro expressing Cre or Vec. (A) Confirmation of deletion of *GCN5* and *PCAF* genes by qRT-PCR. Wild-type MEFs were included as control. (B) Cell morphology under the microscope. (C) Cell growth curves. (D) Deletion of *GCN5* and *PCAF* in MEFs vastly reduces global level of H3K9ac. Nuclear extracts were prepared for western blot analysis of histone acetylations and methylations using indicated antibodies. (E) *GCN5* and *PCAF* are redundant and are required for the global level of H3K9ac. *GCN5*^{fllox/Δ} MEFs and *PCAF*^{-/-}; *GCN5*^{fllox/Δ} MEFs were infected with MSCVpuro expressing Cre. Nuclear extracts were prepared for western blot analysis. (F) *In vitro* HAT assays were performed by incubating 1.5 μg GST-GCN5 protein purified from bacteria or 1 μg GCN5-associated HAT complexes (GCN5.com) purified from MEFs (Supplementary Figure S4) with 1 μg recombinant histone H3 in the presence of acetyl CoA, followed by western blot analyses. Control, mock-purified sample from MEFs. The signals in the GST and the control lanes reflect non-specific detection of recombinant histone H3 by histone acetylation antibodies. All results are representative of two to four independent experiments.

gene expression. Our approach was to delete the two pairs of HATs, GCN5/PCAF and CBP/p300, in MEFs, to study the regulation of endogenous NR target gene activation by histone acetylation.

Before trying to understand the role of GCN5/PCAF-mediated histone acetylation in gene activation, we sought to determine the substrate and site specificities of GCN5/PCAF in cells. Because of the lack of phenotype in *PCAF* null mice (Roth *et al*, 2001), we started with deletion of GCN5 in MEFs. Retroviruses expressing Cre were used to infect the immortalized *GCN5*^{fllox/Δ} MEFs carrying one floxed and one null alleles of *GCN5* (Atanassov *et al*, 2009). Deletion of GCN5 by Cre in MEFs had no significant effect on the global levels of histone acetylations or the GW-induced *Angptl4* expression (Supplementary Figure S2; Figure 3E), suggesting that GCN5 and PCAF could be functionally redundant in MEFs.

Next, we sought to delete both GCN5 and PCAF in MEFs. Primary MEFs were isolated from *PCAF*^{-/-}; *GCN5*^{fllox/Δ} mouse embryos that carried two null alleles of *PCAF* and one floxed and one null alleles of *GCN5*. After immortalization, *PCAF*^{-/-}; *GCN5*^{fllox/Δ} MEFs were infected with retroviral Cre to generate GCN5/PCAF DKO cells. Deletion of GCN5/PCAF was confirmed at both mRNA and protein levels (Figure 3A and E). Interestingly, DKO of GCN5 and PCAF in MEFs had no significant effect on the cell morphology and only slightly

decreased the cell growth rate, indicating that GCN5/PCAF are largely dispensable for the viability and growth of immortalized MEFs (Figure 3B and C). By western blot analysis of histone acetylations and methylations, we found that deletion of GCN5/PCAF in MEFs specifically and dramatically reduced the global level of H3K9ac (Figure 3D). In contrast, single knockout of either GCN5 or PCAF had no effect on the global level of H3K9ac in MEFs (Figure 3E). Western blot in a different type of cells, brown pre-adipocytes, also showed that deletion of GCN5/PCAF dramatically reduced the global level of H3K9ac but not H3K14ac (Supplementary Figure S3A). Using anti-H3K14ac antibodies from two different sources, we confirmed that deletion of GCN5/PCAF had no effect on the global level of H3K14ac in MEFs (Supplementary Figure S3B).

The specific loss of H3K9ac but not H3K14ac or other histone acetylations in GCN5/PCAF DKO cells was surprising, given that the yeast GCN5 and associated SAGA complex are capable of acetylating multiple lysine residues on histone H3 and preferentially acetylate H3K14 over H3K9 *in vitro* (Grant *et al*, 1999). To investigate whether the mammalian GCN5 and associated HAT complexes are capable of acetylating H3K14, we purified recombinant mouse GCN5 from bacteria and affinity-purified GCN5-associated HAT complexes (GCN5.com) from MEFs (Supplementary Figure S4). In the *in vitro* HAT assays using recombinant histone H3 as

Table I Mass spectrometric analysis of the total acetylation levels on H3K9 and H3K14 in retroviral Vec- or Cre-infected *PCAF^{-/-};GCN5^{lox/Δ}* MEFs

Peptide	MH+	ΔM (p.p.m.)	Peak area (× 10 ⁶)		Ratio (Vec/Cre)
			Vec	Cre	
⁹ KSTGG ¹⁴ K _{ac} APR	943.5320	-1.40	534.4	638.6	0.84
⁹ K _{me1} STGG ¹⁴ K _{ac} APR	957.5476	-2.06	541.0	548.0	0.99
⁹ K _{me2} STGG ¹⁴ K _{ac} APR	971.5633	-0.91	1658.7	1956.8	0.83
⁹ K _{ac} STGG ¹⁴ K _{ac} APR	985.5425	-2.22	131.5	6.8	19.26
Sum of ¹⁴ K _{ac}			2865.5	3150.2	0.91

The histone H3 proteins isolated from MEFs were digested with endoproteinase Arg-C to release the ⁹KSTGG¹⁴KAPR peptide encompassing residues K9–R17 of histone H3. The peak area value represents the abundance of each type of modified peptides determined by mass spectrometry, with the relative standard deviation of ~15%. Note that the peptide with acetylation on K9 alone, ⁹K_{ac}STGG¹⁴KAPR, was undetectable. In other words, K9ac was always detected with co-existing K14ac on the same peptide to form ⁹K_{ac}STGG¹⁴K_{ac}APR (H3K9/14ac). Therefore, the total level of H3K9 acetylation (H3K9ac) is represented by the H3K9/14ac level. At the shown high mass measurement accuracy (ΔM (p.p.m.)), tri-methylated and acetylated lysine residues can be distinguished confidently by the mass spectrometer.

substrate, both recombinant mouse GCN5 and GCN5.com strongly acetylated multiple lysine residues on histone H3, including H3K9, H3K14, H3K18, H3K23 and H3K56, with weak acetylations on H3K27 and H3K36 (Figure 3F). These results suggest that mammalian GCN5 and associated HAT complexes are capable of acetylating H3K14, but this acetylation may be compensated by other HATs in GCN5/PCAF DKO cells.

To confirm the western blot results and more importantly, to provide direct evidence that mouse GCN5/PCAF are required for H3K9ac but not H3K14ac in cells, we performed mass spectrometric analysis of the total levels of H3K9ac and H3K14ac on histone H3 protein purified from MEFs (Table I). The data revealed that the total level of H3K14ac (sum of ¹⁴K_{ac} in Table I) was over 20-fold more abundant than that of H3K9ac in MEFs and that H3K9ac always co-existed with H3K14ac on the same histone H3 molecule to form H3K9/14ac (di-acetylation on K9 and K14 of histone H3). Thus, the total H3K9ac level is represented by the H3K9/14ac level in the mass spectrometry data. Infecting *PCAF^{-/-};GCN5^{lox/Δ}* MEFs with retroviral Cre led to over 19-fold decrease of H3K9/14ac level, but had no significant effect on the total level of H3K14ac (Table I). These results provide direct evidence to indicate that GCN5/PCAF are required for H3K9ac, but not H3K14ac in cells. Taken together, western blot and mass spectrometry data demonstrate that mouse GCN5 and PCAF are redundant and are specifically required for the global level of H3K9ac in cells.

GCN5/PCAF and H3K9ac are dispensable for ligand-induced NR target gene expression

We next examined the effects of deletion of GCN5/PCAF and thus the dramatic reduction of H3K9ac on gene expression. Surprisingly, deletion of GCN5/PCAF had little effect on expression of *GAPDH*, *β-actin* and *β-catenin*, although H3K9ac was eliminated on the promoters of these housekeeping genes (Supplementary Figure S3C and D). These results suggest that GCN5/PCAF-mediated H3K9ac is dispensable for housekeeping gene expression in MEFs.

ChIP assays revealed that deletion of GCN5/PCAF in MEFs specifically prevented GW-induced H3K9ac, but had little effect on GW-induced other histone acetylations and methylations on *Angptl4* gene (Figure 4A and B). Deletion of GCN5/PCAF and thus the elimination of GW-induced H3K9ac did not affect the GW-induced recruitment of Pol II on *Angptl4* promoter either (Figure 4C). Consistently, deletion of GCN5/

PCAF had little effect on GW-induced expression of *Angptl4* and other PPARδ target genes in MEFs (Figure 4D). Consistent with the pattern of GW-induced H3K9ac on *Angptl4* promoter (Figure 2C and G), GW induced recruitment of GCN5 and PCAF on *Angptl4* promoter in wild-type MEFs (Figure 4E), which could be blocked by the transcription elongation inhibitor DRB (Figure 4F). These results suggest that GCN5/PCAF are directly responsible for GW-induced H3K9ac on PPARδ target gene promoters and that GCN5/PCAF and GCN5/PCAF-mediated H3K9ac correlate with, but are dispensable for, ligand-induced PPARδ target gene expression in MEFs.

Activation of PPARδ in skeletal muscle induces fat burning and energy expenditure and attenuates metabolic syndrome (Tanaka *et al*, 2003; Evans *et al*, 2004). To investigate whether GCN5/PCAF are required for PPARδ target gene activation in myocytes, *PCAF^{-/-};GCN5^{lox/Δ}* MEFs were infected with retrovirus MSCVpuro expressing MyoD. After puromycin selection, cells were infected with adenoviral Cre, followed by induction of myogenesis. As shown in Supplementary Figure S5A and B, GCN5/PCAF were dispensable for MyoD-stimulated myogenesis and expression of myogenesis markers in MEFs. Further, deletion of GCN5/PCAF had little effect on ligand-induced expression of PPARδ target genes, which are important for fat burning in myocytes (Supplementary Figure S5C).

To investigate whether GCN5/PCAF and GCN5/PCAF-mediated H3K9ac are required for expression of other NR target genes, we treated MEFs with T0901317 and all-trans-retinoic acid, specific ligands for NRs liver X receptor α (LXRα) and retinoic acid receptor α (RARα), respectively (Khetchoumian *et al*, 2007; Lee *et al*, 2008). Deletion of GCN5/PCAF in MEFs prevented ligand-induced H3K9ac on LXRα and RARα target gene promoters, but had little effect on ligand-induced Pol II recruitment to the LXRα and RARα target gene promoters and expression of these genes (Supplementary Figure S6). Taken together, these results suggest that GCN5/PCAF and GCN5/PCAF-mediated H3K9ac correlate with, but are largely if not entirely dispensable for, ligand-induced NR target gene expression.

CBP and p300 are specifically required for H3K18ac and H3K27ac in cells

Our results with GCN5/PCAF DKO MEFs suggested that a different HAT family provides essential co-activator function for PPARδ. We reasoned this might include CBP/p300

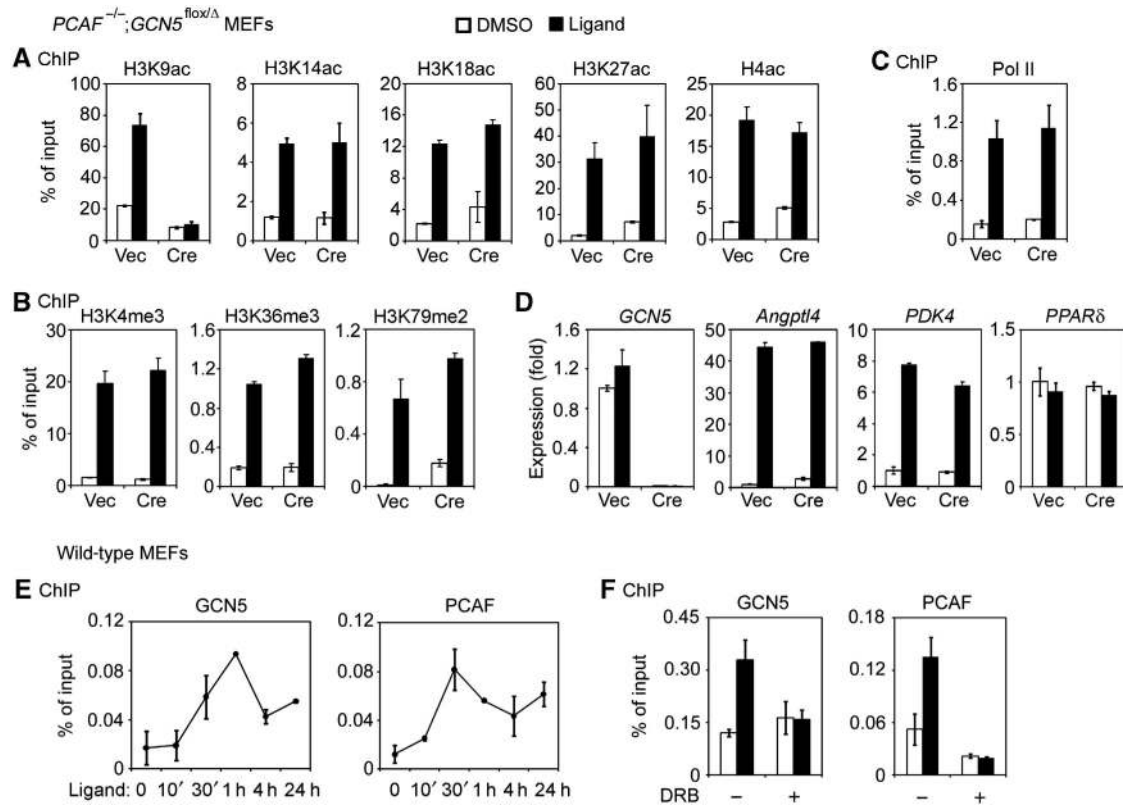


Figure 4 GCN5/PCAF and H3K9ac are dispensable for PPAR δ ligand-induced *Angptl4* expression. (A–D) GCN5/PCAF and GCN5/PCAF-mediated H3K9ac are dispensable for ligand-induced PPAR δ target gene expression in MEFs. *PCAF*^{-/-};*GCN5*^{flox/ Δ} MEFs infected with retroviral Vec or Cre were treated with GW for 24 h, followed by ChIP of histone acetylations (A), methylations (B) and Pol II recruitment (C) on *Angptl4* gene as described in Figure 2. Gene expression was analysed by qRT-PCR (D). (E) Time course of ligand-induced GCN5 and PCAF recruitment on *Angptl4* promoter. Wild-type MEFs were treated with GW. Cells were collected at indicated time points for ChIP of GCN5 and PCAF at the +0.1-kb region on *Angptl4* gene. (F) Wild-type MEFs were pre-treated with DRB for 30 min, followed by treatment with GW for 4 h in the presence of DRB. Cells were collected for ChIP of GCN5 and PCAF at the +0.1-kb region on *Angptl4* gene. All results are representative of two to four independent experiments.

because they are known NR co-activators. To understand how CBP/p300-mediated HAT activities regulate gene expression, we first sought to determine the substrate and site specificities of CBP/p300 in cells. Single deletion of either CBP or p300 in MEFs by retroviral Cre had little effect on the global levels of histone acetylations or the GW-induced *Angptl4* expression (Supplementary Figure S7; Figure 5E), suggesting that CBP and p300 could be functionally redundant.

Next, we immortalized primary *CBP*^{flox/flox};*p300*^{flox/flox} MEFs that carried two floxed alleles of *CBP* and two floxed alleles of *p300*. The immortalized *CBP*^{flox/flox};*p300*^{flox/flox} MEFs were infected with adenoviral Cre to generate CBP/p300 DKO cells. Deletion of CBP/p300 was confirmed at both mRNA and protein levels (Figure 5A and E). In contrast to the deletion of GCN5/PCAF, deletion of CBP/p300 caused marked morphological changes in MEFs. Cells became flat and ceased proliferation after the deletion of CBP/p300, although no significant apoptosis was observed (Figure 5B and C). By western blot, we found that deletion of CBP/p300 in MEFs specifically and dramatically reduced the global levels of H3K18ac and H3K27ac (Figure 5D and E).

To confirm the western blot results and more importantly, to provide direct evidence that CBP/p300 are required for H3K18ac and H3K27ac in cells, we performed mass spectrometric analysis of total levels of H3K18ac and H3K27ac on histone H3 protein purified from MEFs (Table II). The data

revealed that the total level of H3K23ac (sum of ²³K_{ac} in Table II) was about five-fold more abundant than that of H3K18ac in MEFs and that H3K18ac always co-existed with H3K23ac on the same histone H3 molecule to form H3K18/23ac (di-acetylation on K18 and K23 of histone H3). Thus, the total H3K18ac level is represented by the H3K18/23ac level in the mass spectrometry data. H3K27ac always co-existed with H3K36me2 on the same histone H3 molecule. Infecting *CBP*^{flox/flox};*p300*^{flox/flox} MEFs with adenoviral Cre led to 28-fold decrease of H3K18/23ac level and 15-fold decrease of H3K27ac, but had no significant effect on the total level of H3K23ac (Table II). These results provide direct evidence to indicate that CBP/p300 are responsible for over 90% of H3K18ac and H3K27ac in MEFs. Taken together, western blot and mass spectrometry data demonstrate that CBP and p300 are redundant and are specifically required for the global levels of H3K18ac and H3K27ac in MEFs.

CBP/p300 and their HAT activities are essential for ligand-induced NR target gene expression

We next examined the effects of deletion of CBP/p300 and thus the dramatic decreases of H3K18/27ac on gene expression. Deletion of CBP/p300 in MEFs decreased β -actin level by ~40%, but had no effect on expression of other housekeeping genes *GAPDH* and β -catenin (Supplementary Figure S8A). Both H3K18ac and H3K27ac levels decreased

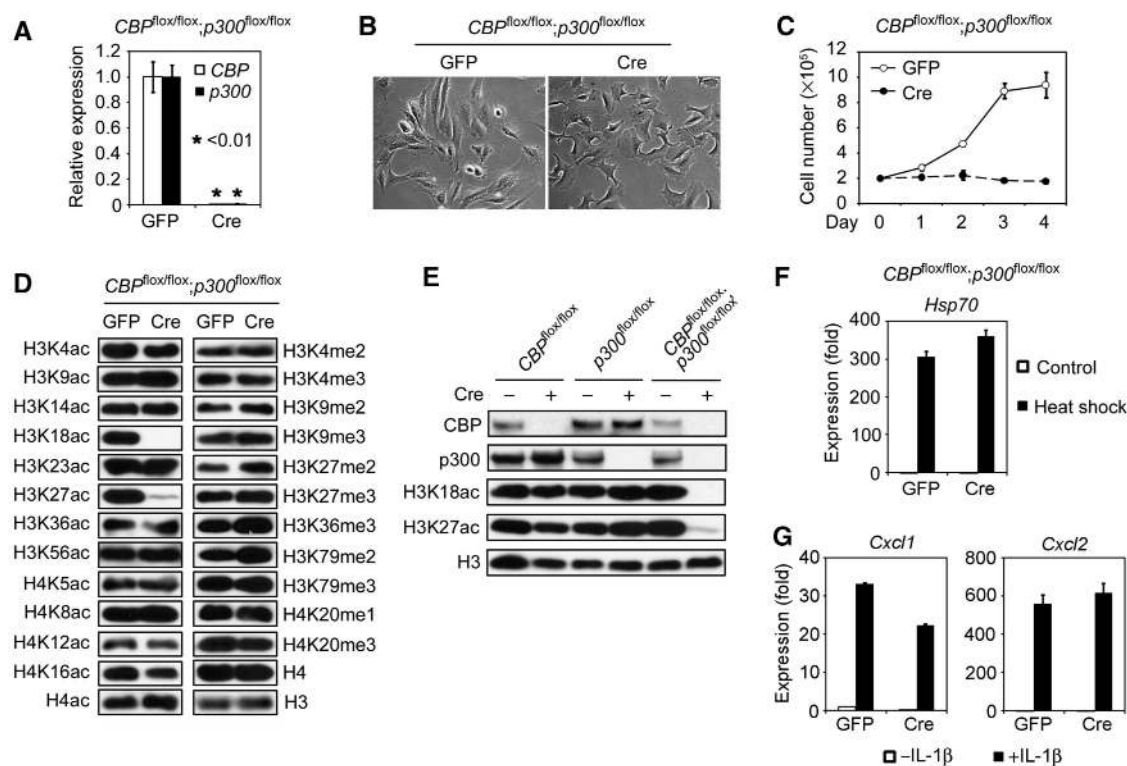


Figure 5 CBP and p300 are redundant and are specifically required for H3K18ac and H3K27ac in cells. Immortalized *CBP^{fllox/fllox};p300^{fllox/fllox}* MEFs were infected with adenoviruses expressing Cre or GFP control. Two days later, cells were re-plated to remove dead cells. After 24 h, cells were subjected to the following analyses. (A) Confirmation of deletion of *CBP* and *p300* genes by qRT-PCR using primers located in deleted regions. (B) Cell morphology under the microscope. (C) Cell growth curves. (D) Deletion of CBP and p300 in MEFs markedly reduces the global levels of H3K18ac and H3K27ac. Nuclear extracts were prepared for western blot analyses of histone acetylations and methylations. (E) CBP and p300 are redundant and are required for the global levels of H3K18ac and H3K27ac. Immortalized *CBP^{fllox/fllox}* MEFs and *p300^{fllox/fllox}* MEFs were infected with retroviruses MSCVpuro expressing Cre or Vec. Nuclear extracts were prepared for western blot analysis. (F) CBP and p300 are dispensable for heat shock-induced *Hsp70* expression. Cells were incubated at 43°C for 30 min, followed by recovery at 37°C for 2 h. (G) CBP and p300 are dispensable for the cytokine interleukin 1β (IL-1β)-induced *Cxcl1* and *Cxcl2* expression. Cells were treated with 10 ng/ml IL-1β for 1 h. All results are representative of two to four independent experiments.

Table II Mass spectrometric analysis of the total acetylation levels on H3K9, H3K14, H3K18, H3K23 and H3K27 in adenoviral GFP- or Cre-infected *CBP^{fllox/fllox};p300^{fllox/fllox}* MEFs

Peptide	MH +	ΔM (p.p.m.)	Peak area (× 10 ⁶)		Ratio (GFP/Cre)
			GFP	Cre	
⁹ KSTGG ¹⁴ K _{ac} APR	943.5320	1.52	1324.5	1264.1	1.05
⁹ K _{me1} STGG ¹⁴ K _{ac} APR	957.5476	0.37	277.4	340.2	0.82
⁹ K _{me2} STGG ¹⁴ K _{ac} APR	971.5633	0.14	1389.3	1414.4	0.98
⁹ K _{ac} STGG ¹⁴ K _{ac} APR	985.5425	0.13	61.5	54.3	1.13
Sum of ¹⁴ K _{ac}			3052.7	3072.9	0.99
¹⁸ KQLAT ²³ K _{ac} AAR	1028.6211	0.87	4239.5	5058.2	0.84
¹⁸ K _{me1} QLAT ²³ K _{ac} AAR	1042.6368	1.19	27.2	48.2	0.56
¹⁸ K _{ac} QLAT ²³ K _{ac} AAR	1070.6317	0.89	1036.9	36.7	28.29
Sum of ²³ K _{ac}			5303.6	5143.1	1.03
²⁷ K _{ac} SAPATGGV ³⁶ K _{me2} KPHR	1503.8754	0.24	20.2	1.3	15.23

The histone H3 proteins isolated from MEFs were digested with endoproteinase Arg-C to release three peptides: the ⁹KSTGG¹⁴KAPR encompassing residues K9–R17, the ¹⁸KQLAT²³KAAR encompassing K18–R26, and the ²⁷KSAPATGGV³⁶KKPHR encompassing K27–R40. The peak area value represents the abundance of each type of modified peptides determined by mass spectrometry, with the relative standard deviation of ~15%. Note that K9ac was always detected with co-existing K14ac on the same peptide to form ⁹K_{ac}STGG¹⁴K_{ac}APR (H3K9/14ac), that K18ac was always detected with co-existing K23ac on the same peptide to form ¹⁸K_{ac}QLAT²³K_{ac}AAR, that K27ac was always detected with co-existing K36me2 on the same peptide to form ²⁷K_{ac}SAPATGGV³⁶K_{me2}KPHR, and that K36ac and K56ac were undetectable.

significantly on the three housekeeping gene promoters in CBP/p300 DKO cells (Supplementary Figure S8B). Deletion of CBP/p300 had little effect on the heat shock-induced *Hsp70* expression and the IL-1β-induced *Cxcl1* and *Cxcl2* expression (Figure 5F and G).

ChIP assays revealed that deletion of CBP/p300 in MEFs prevented GW-induced increases of all histone acetylations and methylations that we have examined on *Angptl4* gene (Figure 6A and B). Deletion of CBP/p300 and thus the elimination of GW-induced H3K18/27ac also prevented

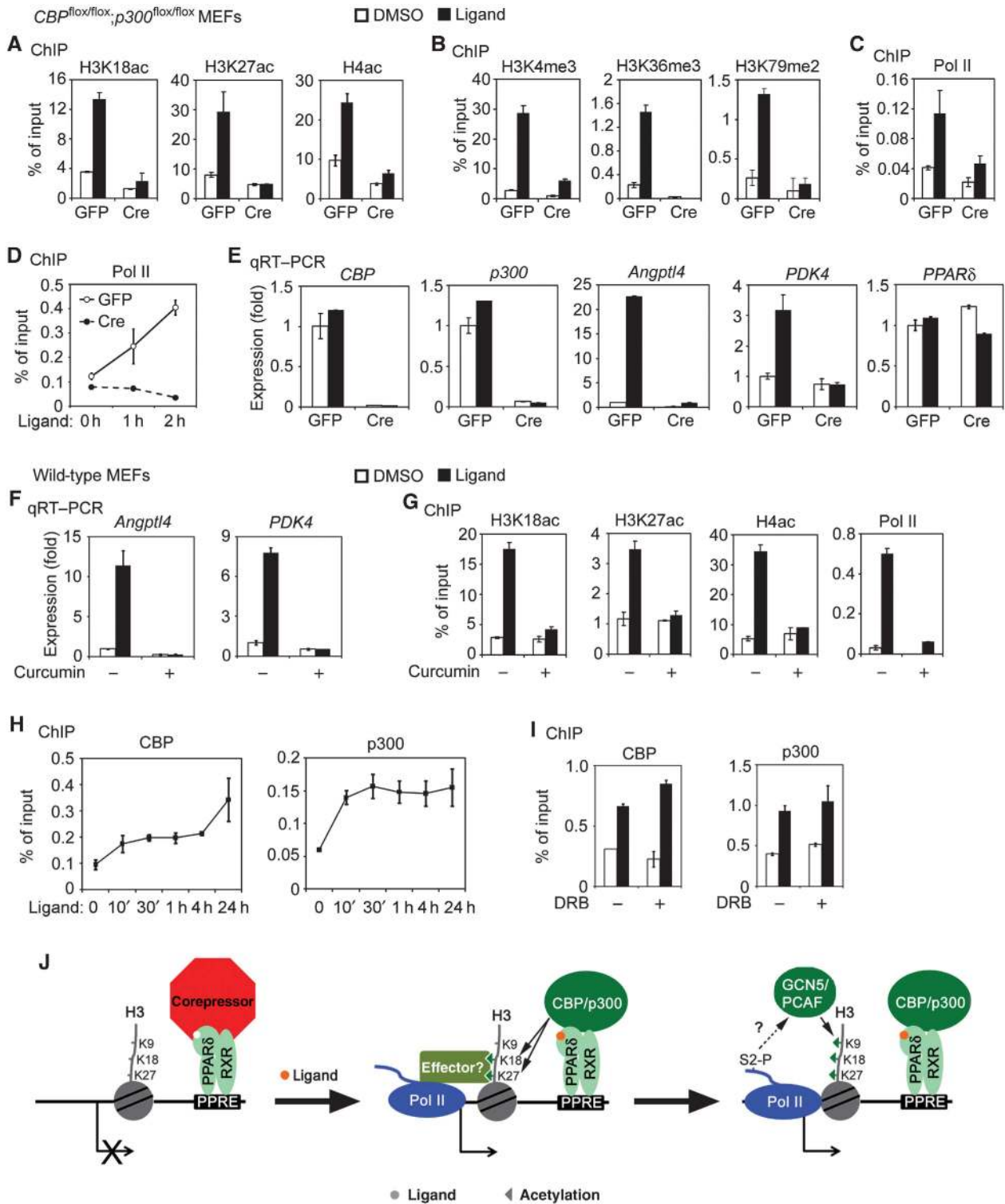


Figure 6 CBP/p300 and their HAT activities are essential for ligand-induced PPAR δ target gene expression. (A, B, C, E) Immortalized *CBP*^{flox/flox}; *p300*^{flox/flox} MEFs were infected with adenoviruses expressing Cre or GFP control. Two days later, cells were re-plated. After 24 h, cells were treated with GW for 24 h, followed by ChIP assays of histone acetylations (A), methylations (B) and Pol II recruitment (C) on *Angptl4* gene as described in Figure 2, as well as qRT-PCR analysis of gene expression (E). (D) Time course of total Pol II recruitment analysed by ChIP. Experiment was done as in C except that cells were treated with GW for 0, 1 and 2 h. (F, G) Wild-type MEFs were treated with GW in the presence of 50 μ M curcumin for 6 h, followed by qRT-PCR analysis of gene expression (F) and ChIP analyses of histone acetylations and Pol II recruitment on *Angptl4* promoter (G). (H) Time course of ligand-induced CBP and p300 recruitment on *Angptl4* gene. Wild-type MEFs were treated with GW. Cells were collected at indicated time points for ChIP analyses of CBP and p300 at the +2.3-kb PPRE on *Angptl4* gene. (I) Wild-type MEFs were pre-treated with DRB for 30 min, followed by treatment with GW for 4 h in the presence of DRB. Cells were collected for ChIP analysis of CBP and p300 at the +2.3-kb PPRE on *Angptl4* gene. (J) Model depicting the distinct roles of GCN5/PCAF-mediated H3K9ac and CBP/p300-mediated H3K18/27ac in NR transactivation, using PPAR δ ligand-induced *Angptl4* expression as an example (see Discussion). All results are representative of two to four independent experiments.

GW-induced recruitment of Pol II on *Angptl4* promoter (Figure 6C and D). Consistently, deletion of CBP/p300 completely prevented GW-induced expression of *Angptl4* and other PPAR δ target genes in MEFs (Figure 6E). Further, treating wild-type MEFs with curcumin, an inhibitor of CBP/p300 HAT activities (Balasubramanyam *et al.*, 2004), inhibited GW-induced H3K18/K27ac and recruitment of Pol II on *Angptl4* promoter, and blocked GW-induced expression of *Angptl4* and other PPAR δ target genes (Figure 6F and G). Consistent with the pattern of GW-induced H3K18/27ac on *Angptl4* promoter (Figure 2C and G), GW induced recruitment of CBP and p300 on *Angptl4* promoter in wild-type MEFs (Figure 6H), which could not be blocked by the transcription elongation inhibitor DRB (Figure 6I). These results suggest that CBP/p300 are directly responsible for GW-induced H3K18/27ac on PPAR δ target gene promoters, and that CBP/p300 and their HAT activities are essential for ligand-induced PPAR δ target gene expression in MEFs.

We also investigated whether CBP/p300 are required for expression of other NR target genes. Deletion of CBP/p300 in MEFs not only prevented ligand-induced H3K18/27ac and Pol II recruitment on promoters of endogenous LXR α and RAR α target genes, but also prevented ligand-induced expression of these genes (Supplementary Figure S9). Taken together, these results suggest that CBP/p300 and CBP/p300-mediated H3K18/27ac are important for ligand-induced NR target gene expression.

Discussion

Histone acetylation generally correlates with gene activation. However, it has been unclear whether the increased histone acetylation is a cause or a consequence of the increased transcription in mammalian cells. Using immortalized GCN5/PCAF DKO cells and CBP/p300 DKO cells, we provide the first systematic examination of the substrate and site specificities of these two distinct families of HATs in mammalian cells. We show GCN5/PCAF and CBP/p300 display remarkable site specificities: GCN5 and PCAF are redundant and are specifically required for over 90% of H3K9ac in cells; CBP and p300 are redundant and are specifically required for over 90% of H3K18ac and H3K27ac (H3K18/27ac) in cells. Determination of the substrate and site specificities of GCN5/PCAF and CBP/p300 in cells makes it possible to understand the molecular mechanism by which these HATs regulate transcription through histone acetylation. Although GCN5/PCAF have been implicated as NR co-activators and H3K9ac is known to correlate well with gene activation, we show for the first time that GCN5/PCAF and H3K9ac are dispensable for ligand-induced activation of endogenous NR target genes. In contrast, CBP/p300 and their HAT activities are critical for ligand-induced histone modifications and Pol II recruitment on NR target gene promoters and gene activation. Thus, GCN5/PCAF-mediated H3K9ac and CBP/p300-mediated H3K18/27ac have distinct roles in NR transactivation. Our data suggest that CBP/p300-mediated H3K18/27ac is important for recruiting Pol II to NR target gene promoters to initiate transcription, while GCN5/PCAF-mediated H3K9ac is dependent on active transcription.

Sequential histone modifications during NR target gene activation

The robust PPAR δ ligand-induced *Angptl4* expression in MEFs is accompanied by ligand-induced marked increases

of histone acetylations, as well as histone methylations that correlate with gene activation such as H3K4me3, H3K36me3 and H3K79me2, on the *Angptl4* gene. These results are consistent with previous genome-wide analyses of histone modifications and studies on regulation of immediate-early gene expression by histone modifications (Edmunds *et al.*, 2008; Wang *et al.*, 2008b). H3K9me2 and H3K27me3 generally correlate with gene repression (Barski *et al.*, 2007). The levels of H3K9me2 and H3K27me3 on *Angptl4* gene are already low before PPAR δ ligand treatment and are not affected by ligand treatment, suggesting that the *Angptl4* gene is pre-disposed for activation and that the two repressive epigenetic marks are not involved in regulating PPAR δ ligand-induced *Angptl4* expression in MEFs.

There appears to be three temporally distinct phases of PPAR δ ligand-induced histone modifications on *Angptl4* gene. The early phase precedes Pol II recruitment and is characterized by rapid increases of H3K14ac, H3K18ac, H3K27ac and H4ac. The intermediate phase is characterized by H3K9ac increase, which coincides with Pol II recruitment and induction of gene expression. The late phase is characterized by increases of H3K4me3, H3K36me3 and H3K79me2 following Pol II recruitment.

The observation that transcription elongation inhibitor DRB blocks the ligand-induced H3K4me3, H3K36me3 and H3K79me2 on *Angptl4* gene is consistent with previous reports that phosphorylation of RNA Pol II mediates histone methylation on H3K4, H3K36 and H3K79 (Hampsey and Reinberg, 2003). Our data that DRB blocks ligand-induced H3K9ac on *Angptl4* promoter imply that the HATs responsible for depositing H3K9ac on NR target genes are neither recruited by NRs before transcription initiation nor important for transcription initiation. Rather, the recruitment of these HATs is transcription dependent. Consistently, we found DRB blocks the ligand-induced GCN5/PCAF and H3K9ac on *Angptl4* gene. In contrast, ligand-induced enrichment of CBP/p300, H3K18ac and H3K27ac on *Angptl4* gene precedes Pol II recruitment and is insensitive to DRB, suggesting that CBP/p300-mediated H3K18ac and/or H3K27ac are important for Pol II recruitment and transcription initiation on NR target gene promoters (see below).

Substrate and site specificities of GCN5/PCAF

Yeast GCN5 and associated SAGA complex are capable of acetylating multiple lysine residues on histone H3 *in vitro*, including H3K9, H3K14, H3K18 and H3K23 (Grant *et al.*, 1999). Both human GCN5/PCAF-associated SAGA and ATAC complexes acetylates histone H3, but not histone H4 *in vitro* (Wang *et al.*, 2008a). Recombinant human GCN5 acetylates H3K9 *in vitro* and knockdown of GCN5 reduced endogenous H3K9ac in human cancer cells (Tjeertes *et al.*, 2009). However, it was unclear whether mammalian GCN5/PCAF are capable of acetylating H3K14ac. Further, the substrate and site specificities of mammalian GCN5/PCAF *in vivo* have not been systematically examined previously.

We show mouse GCN5 and associated HAT complexes are capable of acetylating multiple lysine residues on histone H3 *in vitro*, including H3K9, H3K14, H3K18, H3K23 and H3K56. However, by both western blot and mass spectrometric analyses, we found that deletion of GCN5/PCAF in mouse cells specifically and dramatically reduces the global level of H3K9ac, but has little effect on the global level of H3K14ac or

any other histone H3 and H4 acetylations that we have examined. Consistently, deletion of GCN5/PCAF prevents PPAR δ ligand-induced H3K9ac but not H3K14ac, H3K18/27ac or H4ac on *Angptl4* promoter. It is clear that GCN5/PCAF are critical for both the global and the gene-specific H3K9ac in every species that has been examined. Although we cannot rule out the possibility that GCN5/PCAF may regulate H3K14ac in other cell types in mice, our data suggest that mammalian GCN5/PCAF are capable of acetylating H3K14, but this acetylation may be compensated by other HATs in GCN5/PCAF DKO cells. Alternatively, HATs other than GCN5/PCAF are responsible for H3K14ac in mammalian cells. A potential mammalian H3K14 acetyltransferase is MOZ (also known as Myst3), which is the homologue of the enzymatic Sas3 subunit of the yeast NuA3 complex that preferentially acetylates H3K14 (Taverna *et al*, 2006; Lee and Workman, 2007).

It was recently reported that human GCN5 can acetylate H3K56 *in vitro* and in cells (Tjeertes *et al*, 2009). Mouse GCN5 and associated HAT complexes strongly acetylate H3K56 *in vitro*, but deletion of GCN5/PCAF only leads to mild decrease of H3K56ac in MEFs (Figure 3D and F). Due to its low abundance, we failed to detect H3K56ac even in wild-type MEFs by mass spectrometry. Future work will be needed to determine whether GCN5/PCAF are required for H3K56ac in mammalian cells.

GCN5/PCAF and H3K9ac in NR target gene activation

Our results that GCN5/PCAF and GCN5/PCAF-mediated H3K9ac are dispensable for expression of endogenous NR target genes are surprising, given that GCN5/PCAF are recruited to NR target gene promoters during gene activation and that GCN5/PCAF function as co-activators for several NRs on reporter genes (Blanco *et al*, 1998; Korzus *et al*, 1998; Kraus and Wong, 2002; Metivier *et al*, 2003; Zhao *et al*, 2008). Our study examines the effects of GCN5/PCAF DKO on expression of endogenous NR target genes. In contrast, most of the previous studies that implicate GCN5/PCAF as NR co-activators rely on over-expressing GCN5/PCAF in reporter assays without addressing the contributions from the GCN5/PCAF HAT activities. While we cannot rule out the possibility that GCN5/PCAF may use their HAT activities to function as NR co-activators in a cell type- and/or receptor-specific manner, our data suggest that GCN5/PCAF function as NR co-activators through the associated SAGA and/or ATAC complexes independent of their HAT activities. Such a possibility is supported by results from studies in yeast and *Drosophila* that the GCN5-associated SAGA complex can function as a co-activator independent of its enzymatic activity (Weake *et al*, 2009).

We show that H3K9ac correlates with, but is dispensable for, expression of housekeeping genes and NR target genes. As H3K9ac is a hallmark for gene activation and is enriched on active gene promoters (Wang *et al*, 2008b), these results thus raise an interesting question: what is the role of H3K9ac in transcriptional regulation? We speculate that H3K9ac may help maintain chromatin region permissive for gene expression by preventing the compaction of chromatin, a proposed function for histone acetylation (Roth *et al*, 2001; Li *et al*, 2007). H3K9ac may also be involved in transcriptional memory, although GCN5 is dispensable for transcriptional memory at the yeast *GAL* gene cluster (Kundu *et al*, 2007).

Finally, there remains a possibility that H3K9ac may be redundant with acetylations on other histone lysine residues in regulation of gene expression. Future work will be needed to identify the role of H3K9ac in transcriptional regulation.

Substrate and site specificities of CBP/p300

Using CBP/p300 DKO cells, we systematically examined the substrate and site specificities of CBP/p300 in mammalian cells by western blot and mass spectrometry analyses. We show CBP and p300 are redundant and are specifically required for over 90% of H3K18ac and H3K27ac in MEFs. It has been shown previously that CBP/p300 are capable of acetylating H3K18 and H3K27 *in vitro* and that knockdown of CBP in *Drosophila* S2 cells results in a substantial reduction of H3K18ac and H3K27ac, but has little effect on the global levels of H3K9ac, H3K14ac and H3K23ac (Tie *et al*, 2009). It has also been shown that knockdown of CBP/p300 markedly decreases H3K18ac in human cancer cells and H3K27ac in mouse embryonic stem cells, respectively (Horwitz *et al*, 2008; Pasini *et al*, 2010). The results obtained from our systematic analysis of histone acetylations in CBP/p300 DKO cells are highly consistent with these previous reports.

Depletion of H3K27me2 and H3K27me3 by disrupting the H3K27 methyltransferase PRC2 complex in cells leads to a marked increase of H3K27ac but not H3K18ac (Tie *et al*, 2009; Wang *et al*, 2010), which not only suggests that CBP/p300-mediated H3K27ac antagonizes with PRC2-mediated H3K27me2/3 in regulating polycomb target gene expression, but also suggests that H3K18ac and H3K27ac have overlapping but distinct roles in regulating gene expression. Notably, depletion of H3K27ac by deletion of CBP/p300 in cells only leads to a mild increase of the global H3K27me2 level (Figure 5D). This is probably because H3K27ac and H3K27me2 are mutually exclusive and H3K27ac is enriched around the TSSs while H3K27me2 is broadly distributed (Wang *et al*, 2008b).

It has been reported that CBP/p300 show structural similarity with the yeast H3K56 acetyltransferase Rtt109 and that CBP/p300 are responsible for H3K56ac in human cells (Das *et al*, 2009). By western blot analysis using two different sources of H3K56ac antibodies described in Das *et al* (2009), we found that CBP/p300 are dispensable for H3K56ac in MEFs (Supplementary Figure S8C). On the other hand, we cannot rule out the possibility that CBP/p300 may be required for DNA damage-induced H3K56ac as suggested in Das *et al* (2009).

CBP/p300-mediated H3K18ac and H3K27ac in NR target gene activation

CBP/p300 and their HAT activities are known to be important for ligand-induced activation of several NR target genes (Li *et al*, 2000; Kraus and Wong, 2002). However, due to the previous lack of conclusive evidence on the substrate and site specificities of CBP/p300 in cells, it was unclear how the HATs CBP/p300 regulate NR target gene activation through histone acetylation.

Our determination of the substrate and site specificities of CBP/p300 in cells makes it possible to investigate how this family of HATs regulates transcription through histone acetylation. We show PPAR δ ligand-induced H3K18ac and H3K27ac on *Angptl4* promoter precede Pol II recruitment and cannot be blocked by transcription elongation inhibitor

DRB. However, treating cells with an inhibitor of the CBP/p300 HAT activities block PPAR δ ligand-induced H3K18ac and H3K27ac and recruitment of Pol II to *Angptl4* promoter. These results suggest that CBP/p300-mediated H3K18ac and/or H3K27ac are important for ligand-dependent recruitment of Pol II to NR target gene promoters, although we cannot exclude the possibility that CBP/p300 may acetylate other histone molecules or even non-histone proteins to facilitate Pol II recruitment. CBP/p300 are dispensable for the heat shock-induced *Hsp70* expression and the IL-1 β -induced *Cxcl1* and *Cxcl2* expression, suggesting that the failure in ligand-induced NR target gene expression in CBP/p300 DKO cells is not due to cell growth arrest and that CBP/p300 appear to be selectively required for ligand-induced NR target expression.

Taken together, our data suggest the following model on the distinct roles of CBP/p300-mediated H3K18/27ac and GCN5/PCAF-mediated H3K9ac in NR transactivation, using PPAR δ ligand-induced *Angptl4* expression as an example (Figure 6J). In the absence of ligand, PPAR δ bound on the PPRE motif of the *Angptl4* gene recruits transcription co-repressors to repress *Angptl4* expression (Shi *et al.*, 2002). Ligand binding leads to a conformational change of PPAR δ , which dissociates from co-repressors and associates with CBP/p300 instead. The recruited CBP/p300 specifically acetylate H3K18 and H3K27 on the *Angptl4* promoter. The resulting H3K18/27ac may be recognized by yet to be identified effector proteins, which recruit Pol II to initiate transcription. The serine 2-phosphorylated (S2P) elongating Pol II recruits GCN5/PCAF to specifically acetylate H3K9. The resulting H3K9ac indicates the gene activation status. The candidates for effector proteins that recognize H3K18/27ac would include bromodomain-containing non-histone proteins that specifically recognize acetylated lysine (K) residues (Roth *et al.*, 2001). It remains to be determined whether both H3K18ac and H3K27ac or only one of them are required for recruiting Pol II to initiate transcription of PPAR δ target genes. If both H3K18ac and H3K27ac are required, the likely candidates for effector proteins would include the double bromodomain-containing non-histone proteins (Hargreaves *et al.*, 2009). It will be particularly interesting to isolate and determine the identities of effector proteins that recognize H3K18ac and/or H3K27ac.

Materials and methods

Antibodies and chemicals

All commercial antibodies are listed in Supplementary Table S1 except those indicated specifically in Supplementary Figures S3B and S8C. Anti-p300 antibody for ChIP was described (Kasper *et al.*, 2010). Anti-Ada2a, -Ada2b and -SPT3 antibodies were described (Martinez *et al.*, 2001). Anti-FLAG M2-agarose (A2220), curcumin (C1386) and DRB (D1916) were from Sigma. DRB was dissolved in DMSO and used at 20 μ g/ml. GW501516 (Calbiochem) was dissolved in DMSO and used at 100 nM. IL-1 β (401-ML) was from R&D systems.

Cell culture and virus infection

Cells were routinely cultured in DMEM plus 10% FBS. Primary MEFs were isolated from E12.5 to E14.5 mouse embryos and were immortalized by transfection with a SV40T-expressing plasmid as described (Cho *et al.*, 2007) or by following the 3T3 protocol (Cho *et al.*, 2009).

Retroviral infection of MEFs and MyoD-stimulated myogenesis of MEFs were done as described (Ge *et al.*, 2002). Adenoviruses expressing Cre recombinase and GFP (Ad5CMV-Cre-GFP) or GFP

alone (Ad5CMV-GFP) and adenoviral infection of MEFs was done at 100 moi as described (Cho *et al.*, 2009).

Western blot, qRT-PCR, ChIP and in vitro HAT assay

Western blot and qRT-PCR using Taqman or Sybr Green assays were done as described (Hong *et al.*, 2007; Cho *et al.*, 2009). The sequences of SYBR Green primers are listed in Supplementary Table S2. Data are presented as mean values \pm s.d. ChIP assays of histone modifications were performed as described (Wang *et al.*, 2010). ChIP assays of GCN5/PCAF and CBP/p300 were performed as described in Kasper *et al.* (2010). PCR quantitation of precipitated genomic DNA relative to inputs was performed in duplicate or triplicate using SYBR Green kit. For ChIP on the 6.6-kb mouse *Angptl4* gene, we designed 14 pairs of SYBR Green PCR primers to cover from -10 to +10 kb of the TSS of *Angptl4* gene. The sequences of quantitative PCR primers are listed in Supplementary Table S2.

In vitro HAT assays were performed on 1 μ g recombinant histone H3.1 (New England Biolabs, M2503S) in the presence of acetyl CoA as described (Tie *et al.*, 2009), except that 1.5 μ g recombinant GST-GCN5 or 1.0 μ g GCN5-associated HAT complexes (GCN5.com) were used. GST-GCN5 was purified from bacteria and GCN5.com was purified from nuclear extracts of MEFs expressing FLAG-tagged full-length mouse GCN5 as described (Cho *et al.*, 2007).

Mass spectrometry

Core histones were purified from MEFs using a histone purification kit (Active Motif) and were resolved on 15% SDS-PAGE. The gel was stained with Gelcode Blue Safe Protein Stain (Thermo Scientific). The histone H3 bands were cut out, de-stained and in-gel digested with endoproteinase Arg-C (Roche) that cleaves peptide bonds specifically at the C-terminal side of arginine residues. The resulting peptides were analysed using nanoflow reversed-phase liquid chromatographic separation coupled online to an LTQ-Orbitrap XL mass spectrometer (ThermoFisher) for tandem mass spectrometry (nanoLC-MS/MS). The peptides were loaded onto the LC column for 30 min and then separated at a flow rate of 250 nL/min using a step gradient of 2–42% solvent B (0.1% formic acid in acetonitrile) in 40 min, 42–98% solvent B for 10 min, while mobile phase A was 0.1% formic acid in water. The mass spectrometer was operated in a data-dependent mode to sequentially acquire MS and MS/MS spectra with dynamic exclusion. Normalized collision energy was 35% for MS/MS. The raw MS/MS data were searched using SEQUEST (ThermoFisher) against a protein database including mouse histone H3 with dynamic modifications of Lys acetylation, Lys mono-/di-/tri-methylation, Arg mono-/di-methylation and Met oxidation to identify both modified and unmodified peptides (peptide mass tolerance of 10 p.p.m.). The identified peptides with modifications were further subjected to manual inspection of the peptide sequence and the modification sites by examining the corresponding MS/MS spectra. Extracted chromatographic peak areas of identified peptides were calculated and normalized by the most abundant non-modification peptides to compensate the potential sample amount difference between viral Vec/GFP- and Cre-infected *PCAF*^{-/-}; *GCN5*^{fllox/ Δ} or *CBP*^{fllox/fllox}; *p300*^{fllox/fllox} MEFs. The values of the normalized peak areas represent the abundance of modified peptides in cells.

Supplementary data

Supplementary data are available at *The EMBO Journal* Online (<http://www.embojournal.org>).

Acknowledgements

We thank Y Barak and R Evans for providing *PPAR δ* ^{fllox/fllox} mice, Z Wang and K Zhao for validated histone modification antibodies, R Roeder for Ada2b, SPT3 and Ada2a antibodies, and D Mendrick for critical reading of the paper. This work was supported by the Intramural Research Program of the NIDDK, NIH to KG, NIH R01GM067718 to SYRD and NIH DE018183 to PKB.

Conflict of interest

The authors declare that they have no conflict of interest. The views presented in this article do not necessarily reflect those of the US Food and Drug Administration.

References

- Atanassov BS, Evrard YA, Multani AS, Zhang Z, Tora L, Devys D, Chang S, Dent SY (2009) Gcn5 and SAGA regulate shelterin protein turnover and telomere maintenance. *Mol Cell* **35**: 352–364
- Balasubramanyam K, Varier RA, Altaf M, Swaminathan V, Siddappa NB, Ranga U, Kundu TK (2004) Curcumin, a novel p300/CREB-binding protein-specific inhibitor of acetyltransferase, represses the acetylation of histone/nonhistone proteins and histone acetyltransferase-dependent chromatin transcription. *J Biol Chem* **279**: 51163–51171
- Barski A, Cuddapah S, Cui K, Roh T-Y, Schones DE, Wang Z, Wei G, Chepelev I, Zhao K (2007) High-resolution profiling of histone methylations in the human genome. *Cell* **129**: 823–837
- Bedford DC, Kasper LH, Fukuyama T, Brindle PK (2010) Target gene context influences the transcriptional requirement for the KAT3 family of CBP and p300 histone acetyltransferases. *Epigenetics* **5**: 9–15
- Blanco JCG, Minucci S, Lu J, Yang X-J, Walker KK, Chen H, Evans RM, Nakatani Y, Ozato K (1998) The histone acetylase PCAF is a nuclear receptor coactivator. *Genes Dev* **12**: 1638–1651
- Brownell JE, Zhou J, Ranalli T, Kobayashi R, Edmondson DG, Roth SY, Allis CD (1996) Tetrahymena histone acetyltransferase A: a homolog to yeast Gcn5p linking histone acetylation to gene activation. *Cell* **84**: 843–851
- Chakravarti D, LaMorte VJ, Nelson MC, Nakajima T, Schulman IG, Juguilon H, Montminy M, Evans RM (1996) Role of CBP/P300 in nuclear receptor signalling. *Nature* **383**: 99–103
- Cho Y-W, Hong T, Hong S, Guo H, Yu H, Kim D, Guszczynski T, Dressler GR, Copeland TD, Kalkum M, Ge K (2007) PTIP associates with MLL3- and MLL4-containing histone H3 lysine 4 methyltransferase complex. *J Biol Chem* **282**: 20395–20406
- Cho YW, Hong S, Jin Q, Wang L, Lee JE, Gavrilo O, Ge K (2009) Histone methylation regulator PTIP is required for PPAR γ and C/EBP α expression and adipogenesis. *Cell Metab* **10**: 27–39
- Das C, Lucia MS, Hansen KC, Tyler JK (2009) CBP/p300-mediated acetylation of histone H3 on lysine 56. *Nature* **459**: 113–117
- Dilworth FJ, Fromental-Ramain C, Yamamoto K, Chambon P (2000) ATP-driven chromatin remodeling activity and histone acetyltransferases act sequentially during transactivation by RAR/RXR *in vitro*. *Mol Cell* **6**: 1049–1058
- Edmunds JW, Mahadevan LC, Clayton AL (2008) Dynamic histone H3 methylation during gene induction: HYPB/Setd2 mediates all H3K36 trimethylation. *EMBO J* **27**: 406–420
- Evans RM, Barish GD, Wang YX (2004) PPARs and the complex journey to obesity. *Nat Med* **10**: 355–361
- Ge K, Guermah M, Yuan CX, Ito M, Wallberg AE, Spiegelman BM, Roeder RG (2002) Transcription coactivator TRAP220 is required for PPAR γ 2-stimulated adipogenesis. *Nature* **417**: 563–567
- Grant PA, Eberharter A, John S, Cook RG, Turner BM, Workman JL (1999) Expanded lysine acetylation specificity of Gcn5 in native complexes. *J Biol Chem* **274**: 5895–5900
- Hampsey M, Reinberg D (2003) Tails of intrigue: phosphorylation of RNA polymerase II mediates histone methylation. *Cell* **113**: 429–432
- Hargreaves DC, Horng T, Medzhitov R (2009) Control of inducible gene expression by signal-dependent transcriptional elongation. *Cell* **138**: 129–145
- Hong S, Cho Y-W, Yu L-R, Yu H, Veenstra TD, Ge K (2007) Identification of JmjC domain-containing UTX and JMJD3 as histone H3 lysine 27 demethylases. *Proc Natl Acad Sci USA* **104**: 18439–18444
- Horwitz GA, Zhang K, McBrien MA, Grunstein M, Kurdistani SK, Berk AJ (2008) Adenovirus small e1a alters global patterns of histone modification. *Science* **321**: 1084–1085
- Hummasti S, Tontonoz P (2006) The peroxisome proliferator-activated receptor N-terminal domain controls isotype-selective gene expression and adipogenesis. *Mol Endocrinol* **20**: 1261–1275
- Kamei Y, Xu L, Heinzl T, Torchia J, Kurokawa R, Gloss B, Lin SC, Heyman RA, Rose DW, Glass CK, Rosenfeld MG (1996) A CBP integrator complex mediates transcriptional activation and AP-1 inhibition by nuclear receptors. *Cell* **85**: 403–414
- Kasper LH, Fukuyama T, Biesen MA, Boussouar F, Tong C, de Pauw A, Murray PJ, van Deursen JM, Brindle PK (2006) Conditional knockout mice reveal distinct functions for the global transcriptional coactivators CBP and p300 in T-cell development. *Mol Cell Biol* **26**: 789–809
- Kasper LH, Lerach S, Wang J, Wu S, Jeevan T, Brindle PK (2010) CBP/p300 double null cells reveal effect of coactivator level and diversity on CREB transactivation. *EMBO J* **29**: 3660–3672
- Khetchooumian K, Teletin M, Tisserand J, Mark M, Herquel B, Ignat M, Zucman-Rossi J, Cammas F, Lerouge T, Thibault C, Metzger D, Chambon P, Losson R (2007) Loss of Trim24 (Tif1[α]) gene function confers oncogenic activity to retinoic acid receptor α . *Nat Genet* **39**: 1500–1506
- Korzus E, Torchia J, Rose DW, Xu L, Kurokawa R, McNerney EM, Mullen T-M, Glass CK, Rosenfeld MG (1998) Transcription factor-specific requirements for coactivators and their acetyltransferase functions. *Science* **279**: 703–707
- Kouzarides T (2007) Chromatin modifications and their function. *Cell* **128**: 693–705
- Kraus WL, Kadonaga JT (1998) p300 and estrogen receptor cooperatively activate transcription via differential enhancement of initiation and reinitiation. *Genes Dev* **12**: 331–342
- Kraus WL, Manning ET, Kadonaga JT (1999) Biochemical analysis of distinct activation functions in p300 that enhance transcription initiation with chromatin templates. *Mol Cell Biol* **19**: 8123–8135
- Kraus WL, Wong J (2002) Nuclear receptor-dependent transcription with chromatin. Is it all about enzymes? *Eur J Biochem* **269**: 2275–2283
- Kundu S, Horn PJ, Peterson CL (2007) SWI/SNF is required for transcriptional memory at the yeast GAL gene cluster. *Genes Dev* **21**: 997–1004
- Lee KK, Workman JL (2007) Histone acetyltransferase complexes: one size doesn't fit all. *Nat Rev Mol Cell Biol* **8**: 284–295
- Lee S, Lee J, Lee S-K, Lee JW (2008) Activating signal cointegrator-2 is an essential adaptor to recruit histone H3 lysine 4 methyltransferases MLL3 and MLL4 to the liver X receptors. *Mol Endocrinol* **22**: 1312–1319
- Li B, Carey M, Workman JL (2007) The role of chromatin during transcription. *Cell* **128**: 707–719
- Li J, O'Malley BW, Wong J (2000) p300 requires its histone acetyltransferase activity and SRC-1 interaction domain to facilitate thyroid hormone receptor activation in chromatin. *Mol Cell Biol* **20**: 2031–2042
- Mandart S, Zandbergen F, Tan NS, Escher P, Patsouris D, Koenig W, Kleemann R, Bakker A, Veenman F, Wahli W, Muller M, Kersten S (2004) The direct peroxisome proliferator-activated receptor target fasting-induced adipose factor (FIAF/PGAR/ANGPTL4) is present in blood plasma as a truncated protein that is increased by fenofibrate treatment. *J Biol Chem* **279**: 34411–34420
- Martinez E, Palhan VB, Tjernberg A, Lyman ES, Gamper AM, Kundu TK, Chait BT, Roeder RG (2001) Human STAGA complex is a chromatin-acetylation transcription coactivator that interacts with pre-mRNA splicing and DNA damage-binding factors *in vivo*. *Mol Cell Biol* **21**: 6782–6795
- Metivier R, Penot G, Hubner MR, Reid G, Brand H, Kos M, Gannon F (2003) Estrogen receptor- α directs ordered, cyclical, and combinatorial recruitment of cofactors on a natural target promoter. *Cell* **115**: 751–763
- Oliver WR, Shenk JL, Snaith MR, Russell CS, Plunket KD, Bodkin NL, Lewis MC, Winegar DA, Sznajdman ML, Lambert MH, Xu HE, Sternbach DD, Kliewer SA, Hansen BC, Willson TM (2001) A selective peroxisome proliferator-activated receptor delta agonist promotes reverse cholesterol transport. *Proc Natl Acad Sci USA* **98**: 5306–5311
- Pasini D, Malatesta M, Jung HR, Walfridsson J, Willer A, Olsson L, Skotte J, Wutz A, Porse B, Jensen ON, Helin K (2010) Characterization of an antagonistic switch between histone H3 lysine 27 methylation and acetylation in the transcriptional regulation of Polycomb group target genes. *Nucleic Acids Res* **38**: 4958–4969
- Rosenfeld MG, Glass CK (2001) Coregulator codes of transcriptional regulation by nuclear receptors. *J Biol Chem* **276**: 36865–36868
- Roth SY, Denu JM, Allis CD (2001) Histone acetyltransferases. *Annu Rev Biochem* **70**: 81–120
- Shi Y, Hon M, Evans RM (2002) The peroxisome proliferator-activated receptor delta, an integrator of transcriptional repression and nuclear receptor signaling. *Proc Natl Acad Sci USA* **99**: 2613–2618
- Tanaka T, Yamamoto J, Iwasaki S, Asaba H, Hamura H, Ikeda Y, Watanabe M, Magoori K, Ioka RX, Tachibana K, Watanabe Y,

- Uchiyama Y, Sumi K, Iguchi H, Ito S, Doi T, Hamakubo T, Naito M, Auwerx J, Yanagisawa M *et al* (2003) Activation of peroxisome proliferator-activated receptor delta induces fatty acid beta-oxidation in skeletal muscle and attenuates metabolic syndrome. *Proc Natl Acad Sci USA* **100**: 15924–15929
- Taverna SD, Ilin S, Rogers RS, Tanny JC, Lavender H, Li H, Baker L, Boyle J, Blair LP, Chait BT, Patel DJ, Aitchison JD, Tackett AJ, Allis CD (2006) Yng1 PHD finger binding to H3 trimethylated at K4 promotes NuA3 HAT activity at K14 of H3 and transcription at a subset of targeted ORFs. *Mol Cell* **24**: 785–796
- Tie F, Banerjee R, Stratton CA, Prasad-Sinha J, Stepanik V, Zlobin A, Diaz MO, Scacheri PC, Harte PJ (2009) CBP-mediated acetylation of histone H3 lysine 27 antagonizes Drosophila Polycomb silencing. *Development* **136**: 3131–3141
- Tjeertes JV, Miller KM, Jackson SP (2009) Screen for DNA-damage-responsive histone modifications identifies H3K9Ac and H3K56Ac in human cells. *EMBO J* **28**: 1878–1889
- Wang L, Jin Q, Lee J-E, Su IH, Ge K (2010) Histone H3K27 methyltransferase Ezh2 represses Wnt genes to facilitate adipogenesis. *Proc Natl Acad Sci* **107**: 7317–7322
- Wang Y-L, Faiola F, Xu M, Pan S, Martinez E (2008a) Human ATAC is a GCN5/PCAF-containing acetylase complex with a novel NC2-like histone fold module that interacts with the TATA-binding protein. *J Biol Chem* **283**: 33808–33815
- Wang Z, Zang C, Cui K, Schones DE, Barski A, Peng W, Zhao K (2009) Genome-wide mapping of HATs and HDACs reveals distinct functions in active and inactive genes. *Cell* **138**: 1019–1031
- Wang Z, Zang C, Rosenfeld JA, Schones DE, Barski A, Cuddapah S, Cui K, Roh T-Y, Peng W, Zhang MQ, Zhao K (2008b) Combinatorial patterns of histone acetylations and methylations in the human genome. *Nat Genet* **40**: 897–903
- Weake VM, Swanson SK, Mushegian A, Florens L, Washburn MP, Abmayr SM, Workman JL (2009) A novel histone fold domain-containing protein that replaces TAF6 in Drosophila SAGA is required for SAGA-dependent gene expression. *Genes Dev* **23**: 2818–2823
- Yamauchi T, Oike Y, Kamon J, Waki H, Komeda K, Tsuchida A, Date Y, Li M-X, Miki H, Akanuma Y, Nagai R, Kimura S, Saheki T, Nakazato M, Naitoh T, Yamamura K, Kadowaki T (2002) Increased insulin sensitivity despite lipodystrophy in Crebbp heterozygous mice. *Nat Genet* **30**: 221–226
- Yanagisawa J, Kitagawa H, Yanagida M, Wada O, Ogawa S, Nakagomi M, Oishi H, Yamamoto Y, Nagasawa H, McMahon SB, Cole MD, Tora L, Takahashi N, Kato S (2002) Nuclear receptor function requires a TFIIIC-type histone acetyl transferase complex. *Mol Cell* **9**: 553–562
- Yao TP, Oh SP, Fuchs M, Zhou ND, Ch'ng LE, Newsome D, Bronson RT, Li E, Livingston DM, Eckner R (1998) Gene dosage-dependent embryonic development and proliferation defects in mice lacking the transcriptional integrator p300. *Cell* **93**: 361–372
- Zhao Y, Lang G, Ito S, Bonnet J, Metzger E, Sawatsubashi S, Suzuki E, Le Guezennec X, Stunnenberg HG, Krasnov A, Georgieva SG, Schule R, Takeyama K, Kato S, Tora L, Devys D (2008) A TFIIIC/STAGA module mediates histone H2A and H2B deubiquitination, coactivates nuclear receptors, and counteracts heterochromatin silencing. *Mol Cell* **29**: 92–101